



Cavity ring-down spectroscopy based on a comb-locked optical parametric oscillator source

Z.-T. ZHANG,¹ C.-F. CHENG,^{1,2,*}  Y. R. SUN,^{1,2}  A.-W. LIU,^{1,2}
AND S.-M. HU^{1,2} 

¹Hefei National Laboratory for Physical Sciences at Microscale, iChem Center, University of Science and Technology of China, Hefei 230026, China

²CAS Center for Excellence in Quantum Information and Quantum Physics, University of Science and Technology of China, Hefei 230026, China

*cfcheng@ustc.edu.cn

Abstract: Spectroscopy of molecules in the mid-infrared (MIR) region has important applications in various fields, such as astronomical observation, environmental detection, and fundamental physics. However, compared to that in the near-infrared, precision spectroscopy in the MIR is often limited by the light source and has not shown full potential in sensitivity. Here we report a cavity ring-down spectroscopy system using a tunable narrow-linewidth optical parametric oscillator, which fulfills the requirement of high sensitivity and high precision in the MIR region. The Lamb-dip spectrum of the N₂O molecule at 2.7 μm was measured as a demonstration of spectroscopy in the MIR with kilohertz accuracy.

© 2020 Optical Society of America under the terms of the [OSA Open Access Publishing Agreement](#)

1. Introduction

Precision spectroscopy of molecules, which is a means of investigating subtle effects, plays an important role in modern physics and chemistry [1,2]. For instance, great efforts are devoted to searching the parity violation [3], detecting the electric dipole moment of the electron [4], testing quantum electrodynamics [5], and verifying the stability of fundamental constants [6]. Over the last few decades, molecular spectroscopy has been boosted in terms of precision and sensitivity. The application of optical frequency comb (OFC) [7] and ultra-stable lasers [8] allows scanning the laser frequency with unprecedented precision. Cavity-enhanced methods, such as cavity ring-down spectroscopy (CRDS) [9] and noise-immune cavity-enhanced optical heterodyne molecular spectroscopy (NICE-OHMS) [10], improve the sensitivity by several orders of magnitude, compared with conventional absorption spectroscopy based on multi-pass cells. They have been broadly used in precision spectroscopy and trace detection [11–13].

Fundamental bands of molecules, mostly in the MIR region (400–4000 cm⁻¹), are considered more favorable for precision measurements than overtone bands since they are usually stronger by 1–2 orders of magnitude or even more than the overtones. Moreover, the state density in the MIR region for a polyatomic molecule is significantly lower than that in the near-infrared (NIR). Therefore, the difficulties of assigning and modeling the transitions are reduced. However, laser sources and frequency metrology in MIR are not as convenient as that in NIR. Although precision spectroscopy in MIR has been demonstrated with narrow-linewidth gas lasers [14,15] and quantum cascade lasers (QCLs) [16,17], applications are still limited by relatively narrow tuning range and insufficient sensitivity. Compared to OFCs widely applied in NIR studies, OFC in MIR is still relatively more expensive and inconvenient, which hinders accurate frequency calibration in MIR.

Laser sources based on optical parametric oscillator (OPO) are favorable for precision spectroscopy in the MIR [18–23] since they usually have a broad tuning range of a few thousand

wavenumbers and high output power at the watt level. The frequency calibration of the MIR light (idler) emitted from the OPO source can be implemented by measuring the signal and pump lights with a NIR frequency comb [24]. However, the relatively large linewidth of the OPO sources, typically at the MHz level [20], prevents measurements with higher precision.

Here we report precision spectroscopy based on a broadly tunable narrow-linewidth OPO laser source. A linewidth at the kHz level is achieved by locking both frequencies of the signal and pump lights. A sensitivity (noise equivalent absorption coefficient) of $5.1 \times 10^{-10} \text{ cm}^{-1} \text{ Hz}^{-1/2}$ is obtained by using the cavity ring-down spectroscopy method. As a demonstration, Lamb-dips of two transitions of N_2O at $2.7 \mu\text{m}$ were measured, and the line centers were determined with kHz accuracy.

2. Experimental setup

The optical layout of the OPO-based MIR-CRDS system is shown in Fig. 1. It mainly includes a singly resonant cw-OPO source generating the MIR laser and a sample cell used for cavity ring-down spectroscopy. The OPO laser source has a bow-tie ring cavity, and a 5-cm-long multi-channel MgO:PPLN crystal is placed inside the cavity. The OPO cavity mirrors are highly reflective (>99.9%) at the wavelength range from 1.4 to $1.8 \mu\text{m}$ and transparent at the pump and idler wavelengths. The PPLN crystal is mounted in a copper holder, which is thermal controlled at a preset temperature in the range from 40 to $160 \text{ }^\circ\text{C}$ with a precision of $0.002 \text{ }^\circ\text{C}$, meeting the phase-matching condition. The pump beam from a 1064 nm narrow-linewidth fiber laser is amplified to at most 10 W , then focused on the PPLN crystal in the OPO ring cavity. When the phase-matching condition is fulfilled, the output MIR idler light output power reaches several hundred milliwatts.

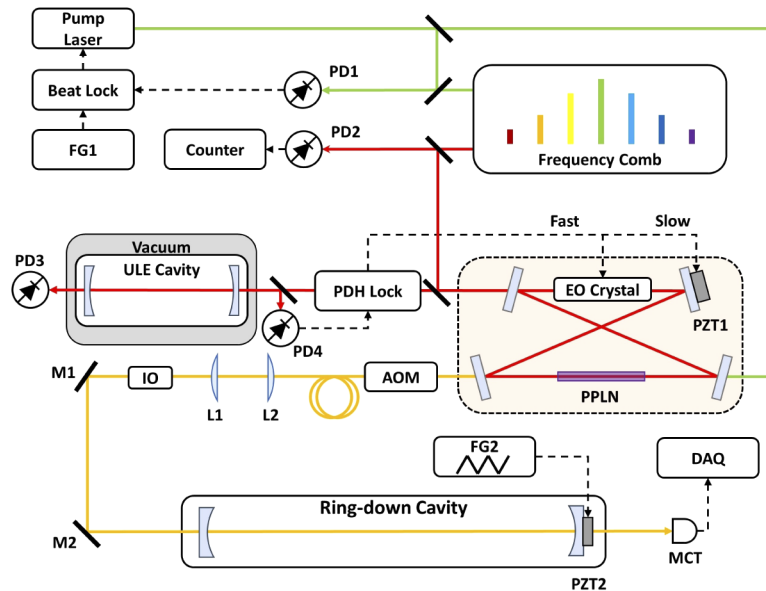


Fig. 1. Scheme of the experimental setup. The green, red and yellow lines indicate pump light, signal light, and idler light, respectively. Abbreviations: PD: photodiode detector; FG: function generator; ULE: ultra-low expansion; PDH: Pound-Drever-Hall; EO Crystal: electro-optical crystal; PZT: piezo actuator; AOM: acoustic-optical modulator; IO: optical isolator; DAQ: data acquisition system; MCT: mercury cadmium telluride detector.

The frequency stabilization of the MIR light is achieved by locking both frequencies of the signal and pump lasers. The pump laser has a manufacturer-specified linewidth of 20 kHz, and its long-term drift is eliminated by locking it to the frequency comb through a beat-lock servo referenced to a function generator (FG1 in Fig. 1). Since the 1064 nm narrow-linewidth pump laser has been well commercialized, the key to control the frequency of the MIR idler light is to lock the frequency of the signal light. The frequency noise of the signal light comes not only from the frequency jitter of the pump laser but also from the mechanical vibration and acoustic noise of the OPO ring cavity. We locked the signal light to an external reference cavity by the PDH method [25]. The reference cavity (FSR = 1.5 GHz, Finesse = 3000 at 1.4 - 1.8 μm) is made of ultra-low expansion (ULE) glass, and the temperature fluctuation is controlled to be less than 0.2 mK. The PDH feedback control signal is divided into two parts: the fast one and the slow one. The fast signal is applied to a home-made electro-optic crystal (EO Crystal in Fig. 1) placed in the OPO cavity. The crystal (15 mm long along the optical axis) is made of LiNbO_3 doped with 3% MgO. The upper and bottom sides of the crystal, parallel to the light plane, have been coated by gold to apply a uniform electric field, while the front and rear surfaces have anti-reflection ($R < 0.2\%$) coatings. The EO crystal is placed in a temperature-stabilized ($\Delta T < 1$ mK) copper housing. The crystal has been carefully installed to avoid stress, which may result in an uncontrollable change in the refractive index. The fast feedback signal from the PDH servo is amplified by a high-voltage amplifier (WMA-300, Falco systems) and then applied on the two gold-coated surfaces of the crystal. The electrical field will modify the refractive index of the crystal, compensating the phase change in the signal light. Currently, the feedback bandwidth reaches 5 MHz, limited by the high-voltage amplifier. The slow signal is applied to a piezoelectric actuator attached to the back of one of the OPO cavity mirrors, changing the signal light frequency by directly adjusting the length of the cavity. In this way, the signal light frequency is stabilized and can be calibrated by monitoring its beat note with the frequency comb.

Fine tuning of the MIR light is implemented by changing the beat-lock reference frequency (FG1 in Fig. 1) of the pump light. Coarse tuning of the MIR light across a large wavelength range is achieved by selecting a polling period and an appropriate temperature of the PPLN crystal to fulfill the quasi-phase-matching conditions. In this setup, the tuning range of the idler light covers the range of 2.6 - 4.5 μm , corresponding to a signal light wavelength in the range of 1.8 - 1.4 μm , and the signal light can be locked to different longitudinal modes of the ULE cavity. When both the signal and pump laser frequencies are locked, the MIR idler frequency (f_{mir}) is determined as,

$$f_{mir} = f_p - f_s - f_{AOM} = (N_p - N_s)f_r + f_{b,p} - f_{b,s} - f_{AOM}, \quad (1)$$

where f_p and f_s are the frequencies of the pump light and the signal light, respectively, f_{AOM} is the AOM frequency shift, N_s and N_p are the comb tooth indices for the pump light and the signal light, respectively, f_r is the comb repetition frequency, $f_{b,p}$ and $f_{b,s}$ are the beat frequencies of the pump light and the signal light with the comb, respectively. Compared to our previous approach using an external laser as the seeding for the signal light [19], the present method is considerably simpler, allowing us to cover a broad range over 1000 cm^{-1} with a single set of optics. The linewidth of the OPO emission is also limited by the mode width of the ULE cavity, which could easily reach the kHz level or less.

The output MIR idler light is collimated and sent to an acoustic-optic modulator (AOM), which serves as a beam chopper for the ring-down measurement. The first-order beam after the AOM is coupled into the ring-down cavity. The ring-down cavity consists of two low-loss and high-reflectivity (HR) concave mirrors ($R > 99.99\%$ at 2.5 - 2.7 μm , Layertec GmbH Inc.). The distance between two mirrors is 65 cm, leading to a free spectral range (FSR) of about 230 MHz. The linewidth of a cavity mode has been measured to be 8 kHz. As shown in Fig. 1, one of the HR mirrors is mounted on a piezo actuator (PZT). The PZT is driven with a 150 Hz triangle wave from a function generator (FG2 in Fig. 1). In this way, a longitudinal mode of

the cavity periodically matches with the frequency of the idler light. A fast TEC-cooled MCT photodetector (PVI-4TE, Vigo system) is used to detect the MIR light transmitted from the cavity. When the signal reaches a preset threshold, the AOM is triggered to cut off the laser and initiates a ring-down event. The ring-down signal is recorded by a data acquisition system, and a fitting program is applied to fit the exponential decay curve yielding the decay time τ . The absorption coefficient could be derived from the following equation:

$$\alpha = \frac{1}{c} \left(\frac{1}{\tau} - \frac{1}{\tau_0} \right), \quad (2)$$

where c is the speed of light, and τ_0 is the decay time of the cavity without sample. Similar cavity ring-down methods at other wavelengths can be found in Ref. [26]. In this experiment, the optic switch has a typical cut-off time of 300 ns, and the decay time of the empty cavity is about 20 μ s.

3. Results and discussion

To determine the linewidth of the signal light, we measured the transfer beat [27] between the signal light and an independent stabilized narrow-linewidth laser at 1.57 μ m. The method allows us to cancel the noise of the frequency comb and obtain a direct beat signal between two lasers. A spectrum of the transfer beat signal recorded in an averaging time of 1 s (256 scans) is shown in Fig. 2(a), where a FWHM linewidth of 22 kHz is determined by fitting with a Lorentzian function. The narrow-linewidth 1.57 μ m reference laser has a Hz-level linewidth, negligible in the transfer beat linewidth. Therefore the 22-kHz linewidth indicates the linewidth of the signal light. As a conservative estimation, the linewidth of the idler laser is less than 30 kHz, which is sufficient for precision spectroscopy measurements of molecules in the MIR region.

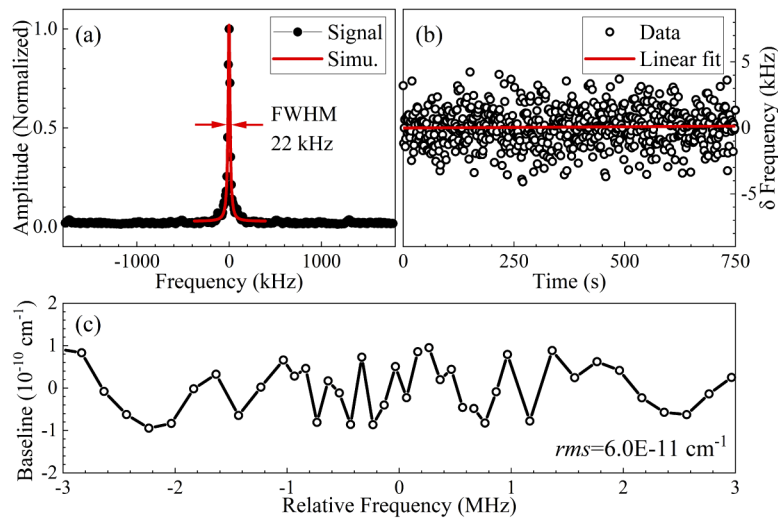


Fig. 2. (a) The spectrum of the transfer beat signal between the OPO signal light at 1.76 μ m and an independent narrow-linewidth laser at 1.57 μ m through an optical frequency comb. (b) Beat frequency between the OPO signal and the frequency comb. (c) A spectrum of the empty ring-down cavity (average of 20 scans obtained in 30 minutes).

As shown in Fig. 2(b), the beat frequency between the signal laser and the frequency comb has been monitored, indicating a long-term frequency drift of the signal laser is less than 1 Hz/s (from linear fitting). The frequency drift comes from the temperature instability and aging of the ULE cavity, which can be monitored and corrected during the spectroscopy acquisition.

To test the sensitivity of the CRDS system, we scanned the laser frequency and recorded the decay time of the empty cavity. A spectrum averaged from 20 scans obtained in 30 minutes is shown in Fig. 2(c), indicating an equivalent minimum detectable absorption coefficient of $6 \times 10^{-11} \text{ cm}^{-1}$.

As a demonstration, saturated absorption spectra of $^{14}\text{N}_2^{16}\text{O}$ lines at $2.67 \mu\text{m}$ were recorded. The measured Lamb dips of R(1)e and P(3)e lines in the $22^0_0-00^0_0$ band at 3749.912 cm^{-1} and 3745.722 cm^{-1} are shown in Figs. 3(a) and (b), respectively. For each line, measurements were taken at four pressures between 0.1 Pa and 0.8 Pa. The spectra were fitted with the Lorentzian profile, and the simulated spectra are shown as solid lines in Fig. 3. Line centers obtained under different pressures are given in Figs. 3(c) and (d). For the R(1)e spectrum at 0.66 Pa, under our experimental conditions, the transit-time broadening is about 270 kHz, the pressure broadening is about 24 kHz [28], and the saturation parameter is about 0.4, leading to a total linewidth (full width at half maximum, FWHM) of 394 kHz. Note that the $^{14}\text{N}_2^{16}\text{O}$ molecule has a hyperfine structure of a few hundred kilohertz [29–31]. The hyperfine splitting is not resolved here but further broadens the line. We simply used the profile with a single Lorentzian peak to fit the spectrum and obtained a linewidth of about 566 kHz.

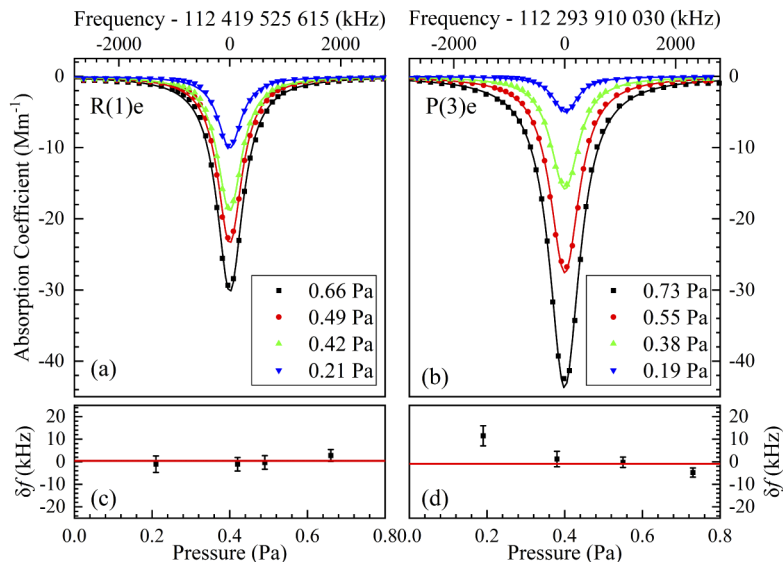


Fig. 3. (a) and (b): Lamb-dip spectra of the R(1)e and the P(3)e transitions in the $22^0_0-00^0_0$ band of $^{14}\text{N}_2^{16}\text{O}$, respectively. Experimental data are shown in scattering dots, and simulated spectra are given in solid lines. (c) and (d): Positions of R(1)e and P(3)e determined from spectra recorded with different sample pressures. The uncertainty due to hyperfine structure and asymmetry in the line profiles was not included in the error bars. Red lines indicate the weighted averages.

The uncertainty budget for the position of the R(1)e in the $22^0_0-00^0_0$ band of $^{14}\text{N}_2^{16}\text{O}$ is given in Table 1. The statistical uncertainty of the line position derived from spectral fitting is about 1 kHz. The frequency comb, which used to calibrate the frequencies of the signal and pump lasers of the OPO system, contributes an uncertainty of 0.66 kHz. The locking servo of the pump laser and the radio-frequency source applied on the AOM each contributes an uncertainty of 0.1 kHz due to environmental temperature drifts. For the $^{14}\text{N}_2^{16}\text{O}$ molecule at room temperature, the second-order Doppler shift is -104 Hz , and the related uncertainty is less than 10 Hz. No obvious pressure induced shift was observed, and we simply use the weighted average of the positions obtained from spectra recorded at different pressures. We also applied a linear fit of the

positions at different pressures and obtained the position at the zero-pressure limit. There is a 4 kHz difference between the two values, which is used as uncertainty for possible pressure induced shift. Note that the $^{14}\text{N}_2^{16}\text{O}$ molecule has a hyperfine structure. According to the hyperfine splittings and relative intensities of the $J = 1 \rightarrow 2$ transition given by Tetenbaum [31], we estimate a 4 kHz shift between the transition center of gravity and the position obtained by fitting with a Lorentzian function. We also include an uncertainty of 10 kHz due to the asymmetry in the observed line profile, which may mainly come from the hyperfine structure. Considering all the corrections and uncertainties given above, we determined the center of the R(1)e line to be 112 419 525 619(11) kHz. Similarly, the center of the P(3)e line is determined to be 112 293 910 030(14) kHz.

Table 1. Uncertainty budget for the position of R(1)e in the 22⁰0-00⁰ band of $^{14}\text{N}_2^{16}\text{O}$ (unit: kHz).

Source	Frequency	Uncertainty	
		Type A	Type B
Statistical	112 419 525 615	1.0	
Comb frequency		0.66	
Pump locking servo		0.1	
AOM frequency		0.1	
Pressure shift			4
2nd-order Doppler	+0.10		0.01
Hyperfine & asymmetry	+4		10
Total	112 419 525 619		11

The R(1)e and P(3)e positions agree with those reported by Toth [32] within two standard deviations, which are 112 419 523(2) MHz and 112 293 907(2) MHz, respectively, and the accuracy has been improved by more than two orders of magnitude. The ground state energy difference between the $J = 1$ and $J = 3$ rotational energy levels is derived from the difference between the R(1)e and P(3)e positions given above, which is 125 615 585(14) kHz. This value agrees with results from microwave spectroscopy [33,34], which are 125 615 609(21) kHz and 125 615 594(16) kHz, respectively. Note that the shift due to hyperfine splittings canceled mostly in the combination difference. Here we did not take into account the uncertainties due to hyperfine splitting and line profile asymmetry, which are also excluded in microwave spectroscopy studies.

4. Summary

In conclusion, we developed a MIR cavity ring-down spectrometer using a comb-locked OPO laser source. The MIR emission from the OPO source covers a wavelength range of 2.6 - 4.5 μm with a linewidth less than 30 kHz. The long-term frequency drift was measured to be at the level of 1 Hz/s. As a demonstration, saturated absorption spectra of two $^{14}\text{N}_2^{16}\text{O}$ lines at 2.7 μm were measured, and the line centers were determined with an accuracy of ten kilohertz, mainly limited by the unresolved hyperfine structure. With the large tuning range and high output power, the OPO source is well suitable for precision measurements of a variety of molecules in the mid-infrared, such as the fundamental vibration of the hydrogen molecule, which could be helpful for investigating the abnormal Lamb-dip profile of the HD transition [35,36]. The sensitivity could be further improved by applying the cavity-locked cavity ring-down spectroscopy method [37–39], which will allow for the optical detection of radiocarbon dioxide [40,41].

Funding

National Natural Science Foundation of China (11974328, 21427804, 21688102); Chinese Academy of Sciences (XDB21020100).

Disclosures

The authors declare no conflicts of interest.

References

1. M. S. Safronova, D. Budker, D. DeMille, D. F. J. Kimball, A. Derevianko, and C. W. Clark, "Search for new physics with atoms and molecules," *Rev. Mod. Phys.* **90**(2), 025008 (2018).
2. T. Steimle and W. Ubachs, "Introduction to the Special issue Spectroscopic Tests of Fundamental Physics," *J. Mol. Spectrosc.* **300**, 1–2 (2014).
3. C. Fábri, L. Horný, and M. Quack, "Tunneling and parity violation in trisulfane (HSSSH): an almost ideal molecule for detecting parity violation in chiral molecules," *ChemPhysChem* **16**(17), 3584–3589 (2015).
4. J. Baron, W. C. Campbell, D. DeMille, J. M. Doyle, G. Gabrielse, Y. V. Gurevich, P. W. Hess, N. R. Hutzler, E. Kirilov, I. Kozyryev, B. R. O'Leary, C. D. Panda, M. F. Parson, E. S. Petrik, B. Spaun, A. C. Vutha, and A. D. West, "Order of magnitude smaller limit on the electric dipole moment of the electron," *Science* **343**(6168), 269–272 (2014).
5. T. M. Trivikram, M. Schlösser, W. Ubachs, and E. Salumbides, "Relativistic and QED Effects in the Fundamental Vibration of T₂," *Phys. Rev. Lett.* **120**(16), 163002 (2018).
6. A. Shelkovich, R. J. Butcher, C. Chardonnet, and A. Amy-Klein, "Stability of the proton-to-electron mass ratio," *Phys. Rev. Lett.* **100**(15), 150801 (2008).
7. T. W. Hänsch, "Nobel Lecture: Passion for precision," *Rev. Mod. Phys.* **78**(4), 1297–1309 (2006).
8. T. Kessler, C. Hagemann, C. Grebing, T. Legero, U. Sterr, F. Riehle, M. Martin, L. Chen, and J. Ye, "A sub-40-mHz-linewidth laser based on a silicon single-crystal optical cavity," *Nat. Photonics* **6**(10), 687–692 (2012).
9. A. O'Keefe and D. A. Deacon, "Cavity ring-down optical spectrometer for absorption measurements using pulsed laser sources," *Rev. Sci. Instrum.* **59**(12), 2544–2551 (1988).
10. J. Ye, L.-S. Ma, and J. L. Hall, "Ultrasensitive detections in atomic and molecular physics: demonstration in molecular overtone spectroscopy," *J. Opt. Soc. Am. B* **15**(1), 6–15 (1998).
11. A. Campargue, S. Kassi, K. Pachucki, and J. Komasa, "The absorption spectrum of H₂: CRDS measurements of the (2-0) band, review of the literature data and accurate ab initio line list up to 35000 cm⁻¹," *Phys. Chem. Chem. Phys.* **14**(2), 802–815 (2012).
12. O. L. Polyansky, K. Bielska, M. Ghysels, L. Lodi, N. F. Zobov, J. T. Hodges, and J. Tennyson, "High-accuracy CO₂ line intensities determined from theory and experiment," *Phys. Rev. Lett.* **114**(24), 243001 (2015).
13. F. M. J. Cozijn, P. Dupré, E. J. Salumbides, K. S. E. Eikema, and W. Ubachs, "Sub-Doppler Frequency Metrology in HD for Tests of Fundamental Physics," *Phys. Rev. Lett.* **120**(15), 153002 (2018).
14. A. Clairon, B. Dahmani, A. Filimon, and J. Rutman, "Precise Frequency Measurements of CO₂/OsO₄ and HeNe/CH₄-Stabilized Lasers," *IEEE Trans. Instrum. Meas.* **IM-34**(2), 265–268 (1985).
15. K. J. Siemsen, J. E. Bernard, A. A. Madej, and L. Marmet, "Absolute frequency measurement of a CO₂/OsO₄ stabilized laser at 28.8 THz," *Appl. Phys. B* **72**(5), 567–573 (2001).
16. I. Galli, S. Bartalini, R. Ballerini, M. Barucci, P. Cancio, M. De Pas, G. Giusfredi, D. Mazzotti, N. Akikusa, and P. De Natale, "Spectroscopic detection of radiocarbon dioxide at parts-per-quadrillion sensitivity," *Optica* **3**(4), 385–388 (2016).
17. S. Borri, G. Insero, G. Santambrogio, D. Mazzotti, F. Cappelli, I. Galli, G. Galzerano, M. Marangoni, P. Laporta, V. Di Sarno, L. Santamaria, P. Maddaloni, and P. De Natale, "High-precision molecular spectroscopy in the mid-infrared using quantum cascade lasers," *Appl. Phys. B* **125**(1), 18 (2019).
18. I. Ricciardi, E. De Tommasi, P. Maddaloni, S. Mosca, A. Rocco, J.-J. Zondy, M. De Rosa, and P. De Natale, "Frequency-comb-referenced singly-resonant OPO for sub-Doppler spectroscopy," *Opt. Express* **20**(8), 9178–9186 (2012).
19. Z.-T. Zhang, Y. Tan, J. Wang, C.-F. Cheng, Y. Sun, A.-W. Liu, and S.-M. Hu, "Seeded optical parametric oscillator light source for precision spectroscopy," *Opt. Lett.* **45**(4), 1013–1016 (2020).
20. J. Peltola, M. Vainio, T. Fordell, T. Hietä, M. Merimaa, and L. Halonen, "Frequency-comb-referenced mid-infrared source for high-precision spectroscopy," *Opt. Express* **22**(26), 32429–32439 (2014).
21. K. N. Crabtree, J. N. Hodges, B. M. Siller, A. J. Perry, J. E. Kelly, P. A. Jenkins II, and B. J. McCall, "Sub-Doppler mid-infrared spectroscopy of molecular ions," *Chem. Phys. Lett.* **551**, 1–6 (2012).
22. M. Vainio, M. Merimaa, and L. Halonen, "Frequency-comb-referenced molecular spectroscopy in the mid-infrared region," *Opt. Lett.* **36**(21), 4122–4124 (2011).
23. T. Hausmaninger, I. Silander, and O. Axner, "Narrowing of the linewidth of an optical parametric oscillator by an acousto-optic modulator for the realization of mid-IR noise-immune cavity-enhanced optical heterodyne molecular spectrometry down to 10⁻¹⁰ cm⁻¹Hz^{-1/2}," *Opt. Express* **23**(26), 33641–33655 (2015).

24. E. V. Kovalchuk, T. Schuldt, and A. Peters, "Combination of a continuous-wave optical parametric oscillator and a femtosecond frequency comb for optical frequency metrology," *Opt. Lett.* **30**(23), 3141–3143 (2005).
25. R. W. P. Drever, J. L. Hall, F. V. Kowalski, J. Hough, G. M. Ford, A. J. Munley, and H. Ward, "Laser phase and frequency stabilization using an optical resonator," *Appl. Phys. B* **31**(2), 97–105 (1983).
26. C.-F. Cheng, Y. R. Sun, H. Pan, J. Wang, A.-W. Liu, A. Campargue, and S.-M. Hu, "Electric-quadrupole transition of H_2 determined to 10^{-9} precision," *Phys. Rev. A* **85**(2), 024501 (2012).
27. H. R. Telle, B. Lipphardt, and J. Stenger, "Kerr-lens, mode-locked lasers as transfer oscillators for optical frequency measurements," *Appl. Phys. B* **74**(1), 1–6 (2002).
28. I. E. Gordon, L. S. Rothman, C. Hill, R. V. Kochanov, Y. Tan, P. F. Bernath, M. Birk, V. Boudon, A. Campargue, K. V. Chance, B. J. Drouin, J.-M. Flaud, R. R. Gamache, J. T. Hodges, D. Jacquemart, V. I. Perevalov, A. Perrin, K. P. Shine, M.-A. H. Smith, J. Tennyson, G. C. Toon, H. Tran, V. G. Tyuterev, A. Barbe, A. G. Császár, V. M. Devi, T. Furtenbacher, J. J. Harrison, J.-M. Hartmann, A. Jolly, T. J. Johnson, T. Karman, I. Kleiner, A. A. Kyuberis, J. Loos, O. M. Lyulin, S. T. Massie, S. N. Mikhailenko, N. Moazzen-Ahmadi, H. S. P. Müller, O. V. Naumenko, A. V. Nikitin, O. L. Polyansky, M. Rey, M. Rotger, S. W. Sharpe, K. Sung, E. Starikova, S. A. Tashkun, J. Vander Auwera, G. Wagner, J. Wilzewski, P. Wcisło, S. Yu, and E. J. Zak, "The HITRAN2016 molecular spectroscopic database," *J. Quant. Spectrosc. Radiat. Transfer* **203**, 3–69 (2017).
29. D. Coles, E. Elyash, and J. Gorman, "Microwave Absorption Spectra of N_2O ," *Phys. Rev.* **72**(10), 973 (1947).
30. M. Sancho and M. D. Harmony, " ^{14}N Quadrupole Coupling Constants in N_2O by High-Resolution Microwave Spectroscopy," *J. Chem. Phys.* **45**(5), 1812–1815 (1966).
31. S. Tetenbaum, "Six-millimeter spectra of OCS and N_2O ," *Phys. Rev.* **88**(4), 772–774 (1952).
32. R. A. Toth, "Line positions and strengths of N_2O between 3515 and 7800 cm^{-1} ," *J. Mol. Spectrosc.* **197**(2), 158–187 (1999).
33. B. A. Andreev, A. V. Burenin, E. N. Karyakin, A. F. Krupnov, and S. M. Shapin, "Submillimeter wave spectrum and molecular constants of N_2O ," *J. Mol. Spectrosc.* **62**(2), 125–148 (1976).
34. H. M. Pickett, R. L. Poynter, E. A. Cohen, M. L. Delitsky, J. C. Pearson, and H. S. P. Müller, "Submillimeter, millimeter, and microwave spectral line catalog," *J. Quant. Spectrosc. Radiat. Transfer* **60**(5), 883–890 (1998).
35. M. L. Diouf, F. M. J. Cozijn, B. Darquié, E. J. Salumbides, and W. Ubachs, "Lamb-dips and Lamb-peaks in the saturation spectrum of HD," *Opt. Lett.* **44**(19), 4733–4736 (2019).
36. T.-P. Hua, Y. R. Sun, and S.-M. Hu, "Dispersion-like lineshape observed in cavity-enhanced saturation spectroscopy of HD at 1.4 μm ," *Opt. Lett.* **45**(17), 4863–4866 (2020).
37. J. Wang, Y. R. Sun, L.-G. Tao, A.-W. Liu, and S.-M. Hu, "Communication: Molecular near-infrared transitions determined with sub-kHz accuracy," *J. Chem. Phys.* **147**(9), 091103 (2017).
38. N. J. van Leeuwen, J. C. Diettrich, and A. C. Wilson, "Periodically locked continuous-wave cavity ringdown spectroscopy," *Appl. Opt.* **42**(18), 3670–3677 (2003).
39. R. Martínez, M. Metsälä, O. Vaitinen, T. Lantta, and L. Halonen, "Laser-locked, high-repetition-rate cavity ringdown spectrometer," *J. Opt. Soc. Am. B* **23**(4), 727–740 (2006).
40. K. K. Lehmann, "Resonance enhanced two-photon cavity ring-down spectroscopy of vibrational overtone bands: A proposal," *J. Chem. Phys.* **151**(14), 144201 (2019).
41. A. J. Fleisher, D. A. Long, Q. Liu, L. Gameson, and J. T. Hodges, "Optical measurement of radiocarbon below unity fraction modern by linear absorption spectroscopy," *J. Phys. Chem. Lett.* **8**(18), 4550–4556 (2017).